Simulation of Millimeter Wave Propagation Characteristics in Indoor Office with Human Blockage at 73GHz Based on Ray Tracing Method

Segni Merga Adula (segnimerga2015@gmail.com)
Haramaya University https://orcid.org/0000-0002-1892-8283
Feyisa Debo Diba
Adama Science and Technology University
Atli Lemma Gebrestadik
Haramaya University

Research Article

Keywords: Millimeter wave, Wideband parameters, Intelligent ray tracing, Propagation

Posted Date: November 10th, 2022

DOI: https://doi.org/10.21203/rs.3.rs-2226946/v1

Simulation of Millimeter Wave Propagation Characteristics in Indoor Office with Human Blockage at 73GHz Based on Ray Tracing Method

Segni Merga

Lecturer

Electrical and Computer Engineering Department

Haramaya University

P.O.Box 138, Dire Dawa, Ethiopia

Email: segnimerga2015@gmail.com,

Tel. +251923391283

Feyisa Debo Diba

Assistant Professor

Department of Electronics & Communication Engineering

School of Electrical Engineering and Computing

Adama Science and Technology University(ASTU)

Email: feyisa2006@yahoo.com

Tel:+251986358573

Atli Lemma

Lecturer of Electrical Engineering

Electrical and Computer Engineering Department

Haramaya University

P.O.Box 138, Dire Dawa, Ethiopia

Email: atli.lemma@outlook.com,

Tel. +251911676673

Fax +2512155530103

Abstract

The modification of current cellular networks, operating in ultra-high frequency (UHF) bands, to support high data rates with optimum coverage is leading to severe bandwidth congestion. As millimeter waves holding large unoccupied bandwidth are among the solutions, an investigation into the wideband characteristics of millimeter wave propagation is paramount. Results from such an investigation can be used for planning and designing indoor 5G wireless communication networks. The main objective of the paper was therefore to simulate and analyze the propagation characteristics of millimeter wave propagation in an indoor complex environment considering the geometry and motion of objects. Intelligent Ray Tracing (IRT) model was employed to predict wideband parameters that affect the propagation of millimeter waves on the second floor of Building-412 of Haramaya University. Propagation considered in this research was mainly from the direct path, single and two-times reflections, and diffraction from moving objects, walls, and indoor objects. The simulation results demonstrated that human shadows near receiver locations significantly obstructed and affected signal strength. Furthermore, the movement of persons in the corridor of the building caused temporal variations of received power, path loss, and delay spread in NLOS. Results were compared with CI path loss model parameters are derived from measurement and indicated that CI path loss model fits the best in indoor environments when compared to other models. As a result, the CI path loss model is chosen to validate the path loss predicted in this paper. This implies that the geometry and motion of objects impact indoor propagation, and hence indoor geometry and motion of objects need to be considered in planning and designing indoor wireless networks.

Keywords Millimeter wave, Wideband parameters, Intelligent ray tracing, Propagation

1. INTRODUCTION

Accurate propagation models are required for gigabit data transmission in millimeter wave frequency bands in order to characterize multipath components, path loss, and shadowing effects. Due to the scarcity of measurement data and suitable channel models for the frequency bands between 8 GHz and 90 GHz, there are a number of issues that require further investigation, including frequency dependence of path loss, multipath delay and angular-spread modelling, massive-array beam forming, and dynamic channel models for adaptive beamforming solutions.

These issues have an impact on data rate, and extensive research is required to obtain full radio propagation characterization [13].Because of its large signal bandwidth, the millimeter wave massive multiple input multiple output (MIMO) channel has been proposed as a promising candidate for cellular Fifth Generation (5G) communication systems. The use of millimeter wave bands in the 5G cellular communication system will result in novel multimedia capabilities. The interaction of waves with various structures is critical in understanding how propagation characteristics change along the bandwidth in the millimeter wave band.

The propagation environment, including buildings and human bodies, must be described in detail. Human presence in indoor scenarios has a significant impact on field level distribution. Electromagnetic fields and waves have difficulty bypassing the human body at millimeter wave frequencies, resulting in moving shadow areas when the body is interrupted between the transmitters and receivers. Attenuation and high blockage loss due to human body and other obstacles found in indoor environments are two of the most important millimeter-wave indoor propagation characteristics. The movement of people, furniture, and the indoor propagation structure in the room causes temporal variations in the indoor propagation characteristics [6]. Other characteristics include strong reflection contributions and multipath channel dispersion.

In [9][10][16] indoor millimeter-wave propagation using the shot and bouncing ray (SBR) method investigated. The transmit and receive antennas are regarded as points in geometry, and the plane symmetry method is used to find the mirror point on the reflection plane that corresponds to the source point, and then the propagation path of rays in space is obtained. The mirror method's complexity grows exponentially with the complexity of the scenario or the order of mirror images, so it can only be used in scenarios with few obstacles and simple geometric shapes. It is incapable of describing and calculating diffraction and scattering. The dense multipath component can be modelled by incorporating one-order or two-order diffuse scattering into ray tracing (RT), which is known as the effective roughness approach. Because RT does not require expensive propagation measurement devices or hard measurement campaigns.

The SBR method was used to study the propagation characteristics of massive MIMO channels in both line of sight (LOS) and non-line of sight (NLOS) outdoor links [17]. The shorter the propagation distance, the earlier the signal arrives and the higher the signal power obtained. The

work did not address the spatial-temporal distribution of mm-wave signals. This work did not investigate the effect of moving (i.e., human) objects on the propagation path and signal.

An overview of 5G propagation models for frequencies up to 100 GHz in indoor offices and shopping malls studied in [5]. The penetration loss is strongly influenced by the material type and thickness. The small-scale channel characteristics, such as delay spread, angular spread, and multipath richness, are similar across a wide frequency range. Clear glass attenuation is 20 dB/cm at 2.5GHz, 3.5 dB/cm at 28GHz, and 11.3 dB/cm at 60GHz, according to the work. Mesh glass penetration increased as a function of frequency, reaching 24.1 dB/cm at 2.5 GHz and 31.9 dB/cm at 60 GHz, and white-board penetration increased as frequency increased. This work did not investigate the effect of moving (i.e., human) objects on the propagation path and signal.

Kim et al. [8] used a wideband MIMO channel sounder with a band-width of 400 MHz at 11 GHz to measure large scale parameters of wide-band multipath channels in various indoor environments. Large-scale parameters such as path loss, shadowing, cross-polarization power ratio, delay spread, and coherence bandwidth, as well as polarization behaviors, were measured and compared. The RMS delay spreads for NLOS and LOS environments were less than 20 and 50 ns, respectively, and the RMS delay spread of cross-polarization was larger than that of co-polarization. The main disadvantage of this model is that its propagation accuracy is low. Because they do not take into account the specifics of the propagation environment.

Al-Samman et al. [4] investigate diffraction loss in indoor propagation channel characteristics at 3.5 GHz and 28 GHz bands using a comparative study. Based on this, the amount of loss due to diffraction from the wall edge in an indoor environment was calculated, and signal degradation was estimated for high frequencies (above 6 GHz) and compared to band frequencies below 6 GHz. In a closed space environment, a wide beamwidth directional antenna is used to cover the entire space of the corridor and pro-vides the same effect as an omni-directional antenna.

The propagation path loss models for frequencies ranging from 2GHz to 73.5GHz over distances ranging from 5m to 1429m presented in [14]. For millimeter frequency bands, the alpha-beta-gamma (ABG) model and the close-in (CI) free space reference distance mode are suitable. Both path loss models are applicable to millimeter and other frequency bands, and they describe large-scale propagation path loss in a specific scenario. The equation for the ABG and CI model given in [16].

$$PL^{ABG}(f,d)[dB] = 10\alpha log_{10}\left(\frac{d}{1m}\right) + \beta + 10\gamma log_{10}\left(\frac{f}{1\ GHz}\right) + X_{\sigma}^{ABG} \quad (1)$$

$$PL^{CI}(f,d)[dB] = FSPL(f,1\ m)[dB] + 10\alpha log_{10}(\mathrm{d}) + X_{\sigma}^{CI} \quad (2)$$

$$FSPL(f,1\ m)[dB] = 20log_{10}\left(\frac{4\pi f}{c}\right) \quad (3)$$

Where $PL^{ABG}(f,d)$ denotes the path loss in dB over frequency and distance, α and γ are coefficients showing the dependence of path loss on distance and frequency, respectively, β is an optimized offset value for path loss in dB, d is the three dimension (3D) transmitter-receiver (T-R) separation distance in meters, f is the carrier frequency in GHz, and $X_{\sigma}^{ABG}$is the SF standard deviation describing large-scale signal fluctuations about the mean path loss over distance. Also, n denotes the single model parameter, the path loss exponent (PLE), with $10n$ describing path loss in dB in terms of decades of distances beginning at 1m, d is the 3D T-R separation distance, and FSPL (f, 1 m) denotes the free space path loss in dB at a T-R separation distance of 1 m at the carrier frequency f and c is the speed of light.

The parameters related to the two path loss model is obtained from measurement data conducted in [11]. The CI path loss model best model to fit when compared with the others model in indoor environments. So, to validate path loss predicted in this paper CI path loss model is selected.

The LOS probability is affected by environment layout and it is frequency-independent. LOS probability predict whether a UE is within a clear LOS or in obstructed NLOS or NLOS region. The 3GPP and ITU LOS probability model developed based on intensive measurements is given by [1][7].

$$InH\ P_{Los} = \begin{cases} 1, & d \le 18 \\ e^{(-(d-18)/27)}, & 18 < d < 27 \\ 0.5, & d \ge 37 \end{cases} \quad (4)$$

Whereas InH indicates indoor hotspot

Root mean square delay spread is related to the characteristic deterioration caused by the inter symbol interference (ISI) and it is the second moment of multipath power delay profile is given by[16][19][18].

$$\sigma_{\tau} = \sqrt{\frac{\sum_{n=1}^{N}\tau_n^2 .P_n}{\sum_{n=1}^{N}P_n} - \left(\frac{\sum_{n=1}^{N}\tau_n .P_n}{\sum_{n=1}^{N}P_n}\right)^2} \quad (5)$$

where σ_τ , P_n and τ_n denote the RMS delay spread, power and excess delay of the n-th multipath respectively.

The electrical properties of the human skin are important for analysis of millimeter wave propagation characteristic in propagation scenarios. The dielectric properties of human skin obtained relative complex permittivity and conductivity [15].

$$\varepsilon^* = \varepsilon' - j\varepsilon'' \quad (6)$$

$$\varepsilon'' = \frac{\sigma}{2\pi f \varepsilon_0} \quad (7)$$

where σ is the conductivity of the material measured in Siemens/meter (S/m), and ε_0 is the permittivity of free space given by 8.85×10^{-12}F/m, f is the operating frequency (Hz).

The rest of the paper is organized as follows. Methodology is described in Section 2. The simulation results are analyzed and discussed in Section 3. Finally, section 4 concludes our findings.

2. METHODOLOGY

To simulate millimeter-wave propagation in indoor scenarios, an office room on the second floor of Haramaya University's HiT Building 412 in Ethiopia was considered, as shown in Fig.1. The simulation scenarios are 30.7 m long and 8.1 m wide, with a partition wall separating the office rooms. Each room varies in size and is equipped with tables and chairs.

Fig.1. Floor plan of simulation scenarios.

To investigate the effect of the human body on millimeter wave propagation, a few humans were randomly disturbed in a corridor and an office while moving at a speed of one meter per second on a pre-defined line, as shown in Fig.2. The simulation is based on snapshots taken at 0s and 3s in indoor environments.

Fig.2. Location of human with respect to Transmitter (Tx) and Receiver (Rx) and direction of moving in corridor and office room at initial position

The interior walls of the office are made of masonry and concrete, and the exterior is covered with brick, clear glass windows, wood doors, and glass on top. The receiver is considered as a mobile terminal and is placed in one of the corridor's locations. As shown in Fig.3, the receiver was only fixed in one position at a height of 1.5 m above the ground.

Table .1: Simulation Parameters

Parameters	**Value**
Operating Frequency	73 GHz
Input (Transmitter) Power	30 dB ,EIRP
Antenna Gain	15.5 dBi
Beam Width	Omni-directional
Transmitter height	2 m
Receiver height	1.5 m

The material properties of buildings have a significant impact on wave propagation within the building. In this scenario, the material properties and wall thickness are essential. Indoor scenarios, on the other hand, contain areas that are difficult to model, such as furniture, moving objects, and other materials. However, have an impact on wave propagation. They attenuate propagation rays by reflecting or diffracting them. Reflected and diffracted characteristics in an indoor environment are affected by polarization, incidence angle, and the material's complex permittivity. The angles-of-arrival of multipath components vary depending on antenna beam widths, building structures, and transmitter and receiver location.

The values presented in Table.2 are embedded in the WallMan or ProMan WinProp tool packages to estimate average received power, path loss, and other parameters in outdoor and indoor office environments. The curve-fitting approach and simple expressions derived in [2][3][12] are used to compute the real part of the relative permittivity, ε', and conductivity (σ).

Table .2: Material properties (Conductivity (σ) and Permittivity (ε')

Materials	Thickness (cm)	Abdullah et al.[3]		Abdulamid etal.[2]		Muttair et al.[12]		Wu et al.[15]	
		σ	Re(ε_γ)	σ	Re(ε_γ)	σ	Re(ε_γ)	σ	Re(ε_γ)
Concrete	50	1.051	5.310	1.051	5.31	1.051	5.310	-	-
Door	5	0.467	1.990	0.466	1.99	0.467	1.990	-	-
Furniture	5								
Glass	2	0.717	6.270	0.716	6.27	-	-	-	-

Metal	3	$10e^7$	1.000	-	-	$10e^8$	1	-	-
Brick	20	0.038	3.750	0.038	3.66	0.038	3.75	-	-
Wall	30	-	-	0.241	2.94	-	-	-	-
Human Body	30	-	-	-	-	-	-	37.73	6.8

3. RESULTS AND DISCUSSION

Radio signals are received in various environments throughout the radio coverage area either through various radio propagation mechanisms. Only in a LOS situation can a radio signal be received directly from the transmitter without encountering obstacles in the propagation environment. Radio signals are reflected or diffracted in other situations, such as NLOS and deep shadowing. Figure 3 depicts the path of a beam transmitted from the transmitter antenna to receiving points in the indoor office corridor scenario. The number of the ray path is set in the WallMan Win Prop package. Materials and moving objects in the building have an unexpected impact on the circulation of the beam.

Fig.3. Propagation Path from Tx to Rx in 3D view at initial position

The greater the number of interactions considered, the better the accuracy of predictions and the longer the computation time. This is true only until the optimal number of interactions is considered. The number of ray interactions with obstacles is determined by the distance between the transmitter and receiver, as well as the density of obstacles, among other factors. To reduce computational complexity, the maximum number of propagation paths used in the simulation is set to 20. For the computation of predictions, two reflections and one diffraction are sufficient. The number of propagation paths influences the strength of the received signal. Most multi propagation paths are present in scenarios when the received signal increases. Figure 3 illustrates the effect of the human body on millimeter wave propagation. The received power decreases as the distance from the transmitting antenna increases.

Furthermore, power degradation in the NLOS regions was caused by reflections and diffraction caused by the building structure and human body found in the corridor.

3.1. Received Power

The received power is lower than the signal power received after 3 seconds of snapshot time, according to the simulation result at initial position (0s). Because only a few rays are reflected by the human body, and Rx is located in NLOS. When the person moved to the transmitter as shown in Fig.5, the Rx placed LOS after 3 seconds with a signal level of -64.34 dBm.

Table 3: Status of Rx at 0s and 3s snapshot

Parameters	**At t = 0s**	**At t = 3s**
LOS Status of Rx	NLOS	LOS
Received Power (dBm)	-68.89	-64.34
Delay Spread (ns)	583.11	160.39

Indoor power distribution differs from outdoor power distribution. Because of the structure of buildings and moving objects, propagation distance in LOS is very short in indoor scenarios. In the initial positions, the receiver points Rx in NLOS. As shown in Fig. 4, the shadowing is affected by the size, shape, and location of the humans.

Fig.4. Received power distribution at 0s (left) and 3s (right) snapshot.

The corridor has the highest average signal distribution and the highest signal attenuation in an office room. The power signal decreases as the thickness of the wall increases. As a result, when there are walls in the signal path, the signals in the office suffer significantly. The received signal in the NLOS room is the result of reflections and diffraction from many humans in the corridor and on the wall.

As shown in Fig.5, power distribution varies throughout the office corridor, with received power varying from -71.39 dBm to -48.44 dBm and -69.09 dBm to -48.34 dBm at the initial and after 3seconds snapshots, respectively.

Fig.5. Received power comparison at 0s and 3s time snapshot with free space models

The propagation path is obstructed by the human body at 13.5 m of Tx-Rx separation distance, and signal power is reduced to - 71.39 dBm at the initial position, as shown in Fig.5. There is a significant difference between two snap-shot times after this separation distance.

3.2. Delay Spread

Radio waves arrive at the receiver through various paths of propagation rays, each with its own arrival time and power strength. This will result in the delay spreading. Multipath propagation is one of the fundamental phenomena affecting the quality of received signals in an indoor environment, causing significant dispersions in the time and angular domains.

Fig.6. Delay Spread 3D distribution in indoor at 0s (left) and 3s (right) snapshot

Inter-symbol interference is caused by delay spread, limiting the maximum transmission rate. At Rx points, long-delayed rays are predicted. Rays with long delays could be the reason for the indoor office structure, people on the corridor, and location Tx and Rx. This ray's contribution to received power is minimal, but it does contribute to a large delay spread. Rays with long delays are observed, resulting in a large delay spread at two different simulation times. The corresponding delay spread differs due to the difference in the number of rays received.

Fig.7. Delay spread comparisons at different time snapshot

This paper simulates the delay spread at 73 GHz using the ray tracing method at various snapshots while taking into account the impact of moving objects in the corridor. For Tx-Rx separation distance, the predictions of delay spread at snapshots of 0s and 3s are shown in Fig.7. As shown in Fig.12, the predicted delay spread for the snap-shot at 3s and 0s in the selected Tx-Rx separation distance ranges from 173.89 ns to 561.26 ns and 0 ns to 361.12 ns. As shown in Fig.7, the minimum delay is predicted in the initial position (0s snapshot at 13m from the transmitter on Tx-Rx separation). This is due to human obstruction on the corridor.

3.3. Path Loss

Fig.8. Path Loss predicted at different snapshot and based on CI LOS models

Figure 8 shows the predicted path loss over separation distances for NLOS scenarios at 73 GHz mm-wave. The path loss increases as the Tx-Rx separation distance in-creases. However, the rate of increase varies depending on the Tx-Rx separation distance. At 13.5 m, the transmitted signal is obstructed by humans in the initial positions. However, the location of humans at this point changes after 3 seconds. The signal path is affected at some points of prediction due to the presence of obstacles and shadow (humans). The CI path loss model parameters are derived from measurement data collected in [11]. The CI path loss mod-el fits the best in indoor environments

when compared to other models. As a result, as shown in Fig.8, the CI path loss model is chosen to validate the path loss predicted in this paper.

3.4. Power Delay Profile

The number of rays arriving at prediction points differs significantly in terms of delay spread and power level be-tween the two snapshot times. As shown in Fig.9, the maximum excess delay for all received paths at Rx with -104.37 dBm power level at initial snapshot positions is 2651.02ns. The receiver is in the NLOS path at the time of this snapshot. As shown in Fig.10, the majority of power falls into the LOS path after a 3-second snapshot, with a maximum power of -68.93 dBm. The receiver Rx appears in the LOS path with a maximum excess delay of less than 1330.54 ns.

Many paths in NLOS have a greater delay than in LOS conditions. At the initial positions of the snapshot, a high power delay profile was observed. Human movement, which could have served as absorbers to reduce the power of most low-delay multipath components. There are only a few paths that have a large delay spread.

Fig.9. Power delay profile predicted at 0s

Fig.10. Power delay profile predicted at 3s

4. CONCLUSIONS

The study of millimeter wave propagation is critical for the design and planning of future indoor wireless communication networks. Accurate propagation characteristics, among other factors, are required for optimal indoor transmitter placement. The human body and the structure of the indoor office have an impact on millimeter wave propagation. The movement of objects within the room causes temporal variations and deterioration of the received power, path loss, and unexpected delay spread in. The strength of the signal decreases as the thickness of the wall and the positions of moving objects change. The received signal predicted in NLOS in this paper is the result of reflections and diffraction from various building materials. In NLOS, a high power delay profile was observed. All of these factors influence millimeter wave propagation and make it more difficult to precisely describe millimeter wave propagation characteristics in complex indoor offices.

5. DECLARATION

Funding

There is no grant funding received for this research.

Conflict of Interest

We declare that there is no conflict or competing interests related to the conduct, methodology, and results of this research

Availability of Data and Materials

The data generated and associated materials in this research can be availed when requested.

Code Availability

We have used the commercial software known as WinProp with built in WallMan and ProMan. We have not written any custom code. However, we have configured and used the software to meet our needs.

6. ACKNOWLEDGMENT

We would like to thank Haramaya University for providing funding for this research. Specially, we would like to thank the School of Graduate Studies of the University.

LIST OF ABBREVATION

3D- Three dimension
5G – Fifth Generation
ABG- alpha-beta-gamma
CI - close-in
dB-Decibel
FSPL- Free space path loss
IMT - International Mobile Telecommunications
ISI- intersymbol interference
ITU –International telecommunication Union
LOS-Line of sight
MIMO- multi input multi output
NLOS –Non line of sight
PLE-Path loss exponent
RMS-Root mean square
RT-Ray tracing
SBR- Shoot and bouncing ray
UE-User Equipment

3. REFERANCES

1. 3GPP, (2015). Study on 3D channel model for LTE, Technical report. 3GPP 36.873V12.2.0

2. Abdulwahid, M. M., Al-Ani, O. A. S., Mosleh, M. F.& Abd-Alhameed, R. A. (2019). Investigation of millimeter-wave indoor propagation at different frequencies. *In 2019 4th Scientific International Conference Najaf (SICN),* (pp.25-30). IEEE.
3. Al Abdullah, A. A., Ali, N., Obeidat, H., Abd-Alhmeed, R. A. & Jones, S. (2017). Indoor millimetre-wave propagation channel simulations at 28, 39, 60 and 73 GHz for 5G wireless networks. *In 2017 Internet Technologies and Applications (ITA)*, (pp.235-239). IEEE.
4. Al-Samman, A. M., Al-Hadhrami, T., Daho, A., Hindia, M. H. D., Azmi, M. H., Dimyati, K & Alazab, M. (2019). Comparative study of indoor propagation model below and above 6 GHz for 5G wireless networks. *Electronics*, Vol 8(1):44.
5. Haneda, K., Zhang, J., Tan, L., Liu, G., Zheng, Y., Asplund, H &Ghosh, A.(2016). 5G 3GPP-like channel models for outdoor urban microcellular and macrocellular environments. *In 2016 IEEE 83rd vehicular technology conference (VTC spring)*,(pp.1-7). IEEE.
6. ITU-R (International Telecommunication Union Recommendation). (2017). Prediction Methods for the Planning of Short-Range Outdoor Radio Communication Systems and Radio Local Area Networks in the Frequency Range 300 MHz to 100 GHz. *International Telecommunication Union: Geneva, Switzerland*.
7. ITU-R (International Telecommunication Union Recommendation), M. (2010). Guidelines for evaluation of radio interface technologies for IMT-Advanced.
8. Kim, M. D., Liang, J., Kwon, H. K. & Lee, J. 2015. Directional delay spread characteristics based on indoor channel measurements at 28GHz. In *2015 IEEE 26th Annual International Symposium on Personal, Indoor, and Mobile Radio Communications (PIMRC)*, (pp.403-407). IEEE.
9. Li, S., Liu, Y., Lin, L., Wang, M., Sheng, Z & Sun, D. (2017). Millimeter-wave propagation measurement and simulation in an indoor office environment at 28 GHz. In *2017 Sixth Asia-Pacific Conference on Antennas and Propagation (APCAP)*, (pp.1-3). IEEE.
10. Li, S., Liu, Y., Lin, L., Sun, X., Yang, S & Sun, D. (2018). Millimeter-Wave channel simulation and statistical channel model in the cross-corridor environment at 28 GHz for 5G wireless system. In *2018 International Conference on Microwave and Millimeter Wave Technology (ICMMT)*,(pp.1-3). IEEE.
11. Maccartney, G. R., Rappaport, T. S., Sun, S., & Deng, S. (2015). Indoor office wideband millimeter-wave propagation measurements and channel models at 28 and 73 GHz for ultra-dense 5G wireless networks. *IEEE access*, Vol *3*, (pp.2388-2424).
12. Muttair, K. S., Al-Ani, O. A. S. & Mosleh, M. F.(2019). Outdoor Millimeter-Wave Propagation Simulation Model for 5G Band Frequencies. In *2019 2nd International Conference on Electrical, Communication, Computer, Power and Control Engineering (ICECCPCE)*, (pp.40-45). IEEE.
13. Salous, S., Degli Esposti, V., Fuschini, F., Thomae, R. S., Mueller, R., Dupleich, D. & Nekovee, M. (2016). Millimeter-Wave Propagation: Characterization and modeling toward fifth-generation systems. [Wireless Corner]. *IEEE Antennas and Propagation Magazine*, Vol.*58*(6), (pp.115-127).

14. Sun, S., Rappaport, T. S., Rangan, S., Thomas, T. A., Ghosh, A., Kovacs, I. Z. & Jarvelainen, J. (2016). Propagation path loss models for 5G urban micro-and macro-cellular scenarios. In *2016 IEEE 83rd Vehicular Technology Conference (VTC Spring)*, (pp.1-6). IEEE.
15. Wu, T., Rappaport, T. S. & Collins, C. M. (2015). The human body and millimeter-wave wireless communication systems: Interactions and implications. *In 2015 IEEE International Conference on Communications (ICC)*, (pp.2423-2429). IEEE.
16. Yang, S., Liu, Y., Li, S. & Sun, D. (2018). Simulation and Analysis of 60 GHz Millimeter Wave Propagation Characteristics in Laboratory Environment. In *2018 International Conference on Microwave and Millimeter Wave Technology (ICMMT)*, (pp.1-3). IEEE.
17. Yao, L., Liu, Y. & Li, S.(2019). Study on Propagation Characteristics of Outdoor Massive MIMO Channel Based on the SBR Method. In *2019 International Conference on Microwave and Millimeter Wave Technology (ICMMT)*, (pp.1-3). IEEE.
18. Yi, H., Guan, K., He, D., Ai, B., Dou, J. & Kim, J.2019. Characterization for the vehicle-to-infrastructure channel in urban and highway scenarios at the terahertz band. *IEEE Access*, Vol 7, (pp.166984-166996).
19. Zhang, X., Liu, Y., Li, S. & Wang, G. (2016). Simulation of 38 GHz millimeter-wave propagation characteristics in the indoor environment. In *2016 IEEE International Conference on Ubiquitous Wireless Broadband (ICUWB)*, (pp.1-3). IEEE.

Figures

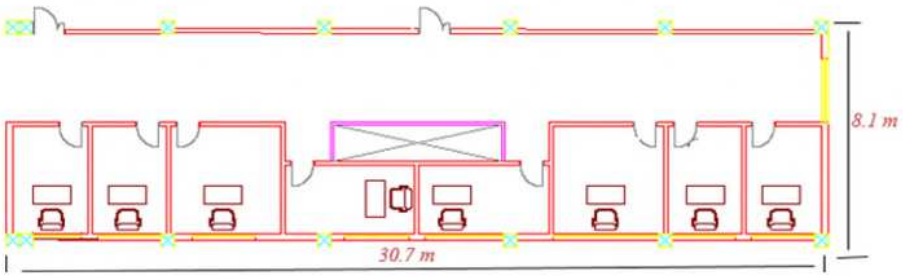

Figure 1

Floor plan of simulation scenarios.

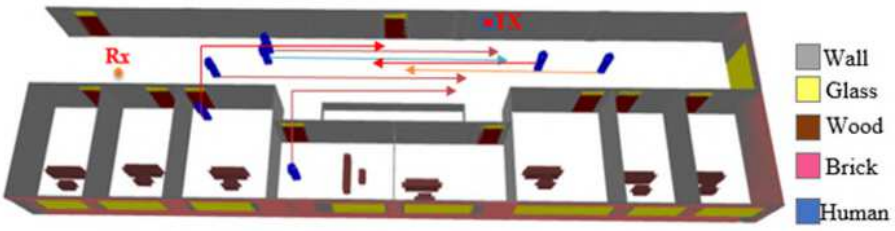

Figure 2

Location of human with respect to Transmitter (Tx) and Receiver (Rx) and direction of moving in corridor and office room at initial position

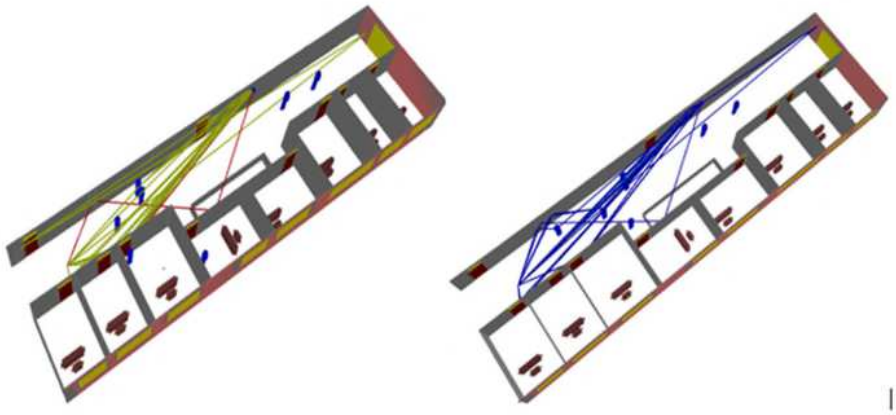

Figure 3

Propagation Path from Tx to Rx in 3D view at initial position

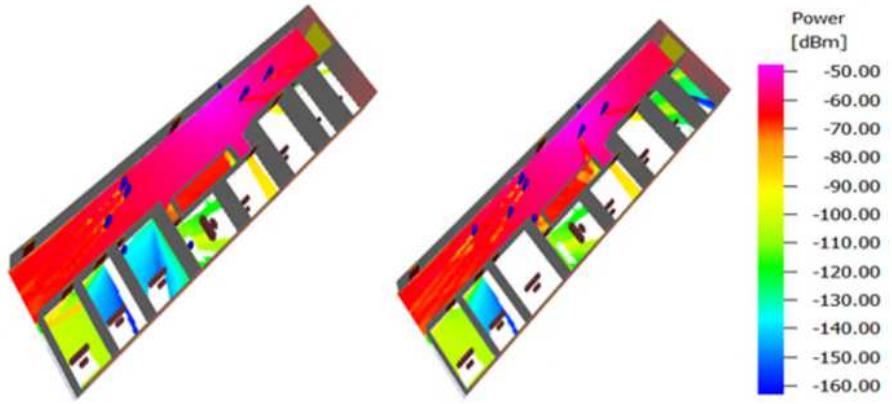

Figure 4

Received power distribution at 0s (left) and 3s (right) snapshot.

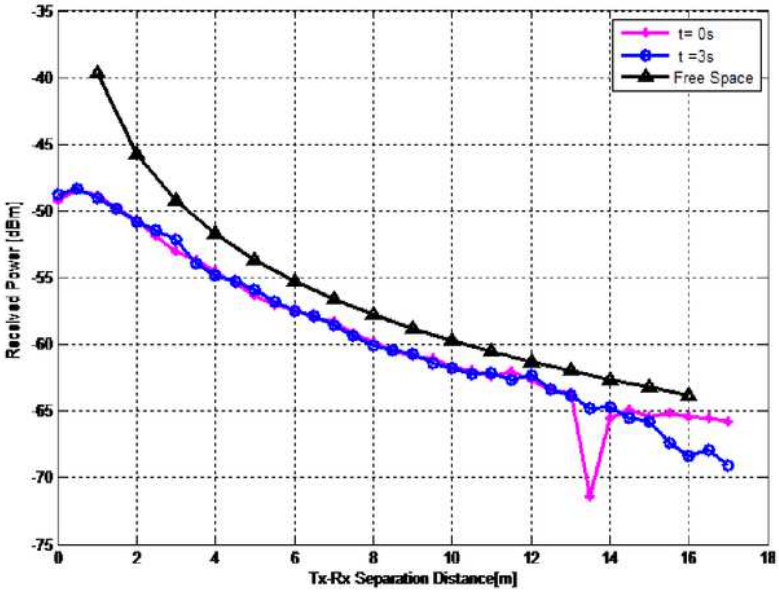

Figure 5

Received power comparison at 0s and 3s time snapshot with free space models

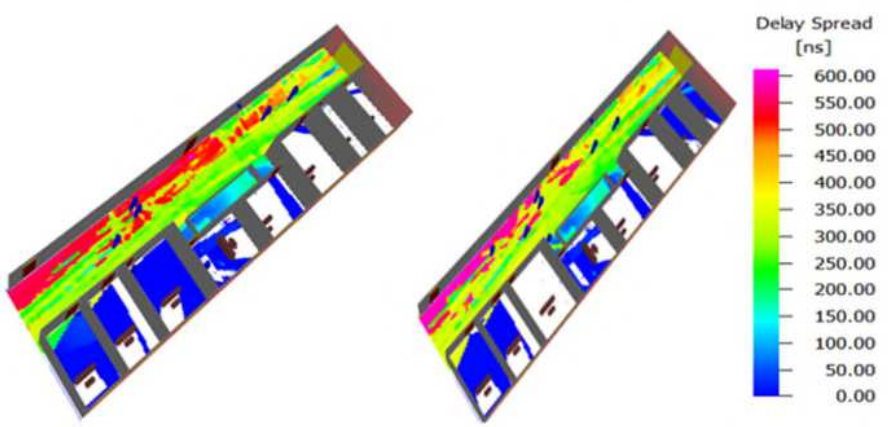

Figure 6

Delay Spread 3D distribution in indoor at 0s (left) and 3s (right) snapshot

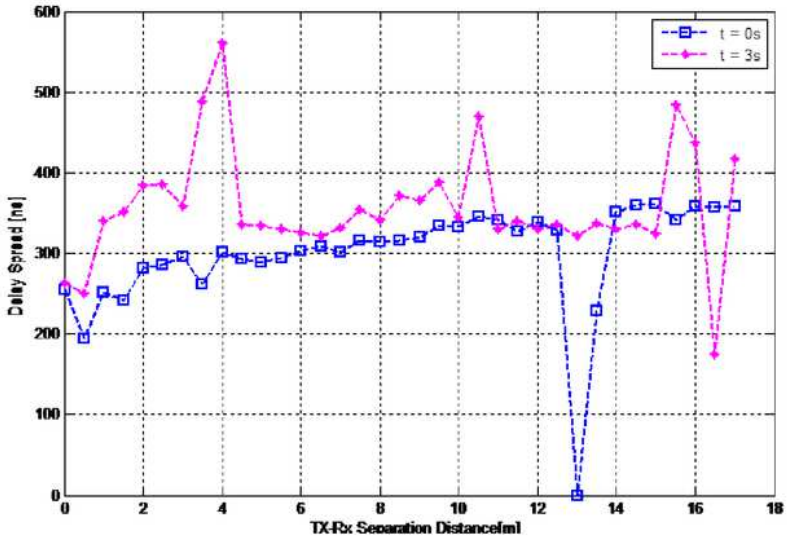

Figure 7

Delay spread comparisons at different time snapshot

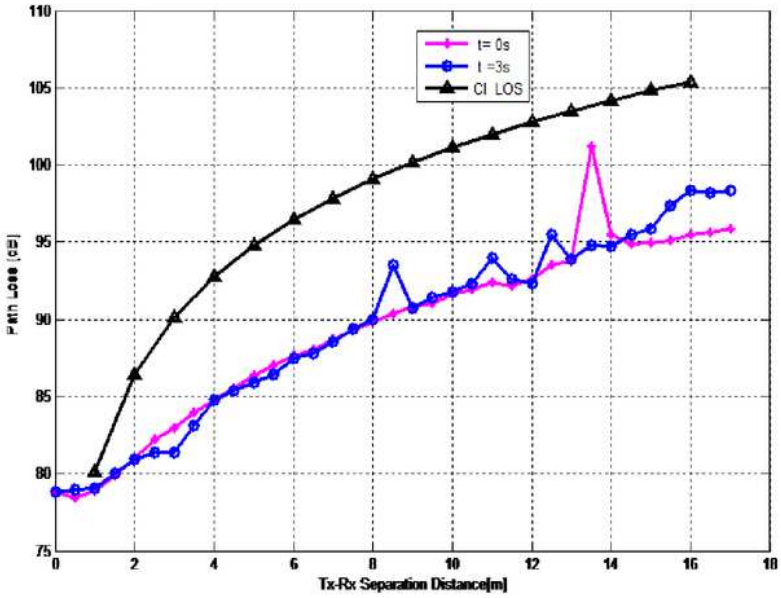

Figure 8

Path Loss predicted at different snapshot and based on CI LOS models

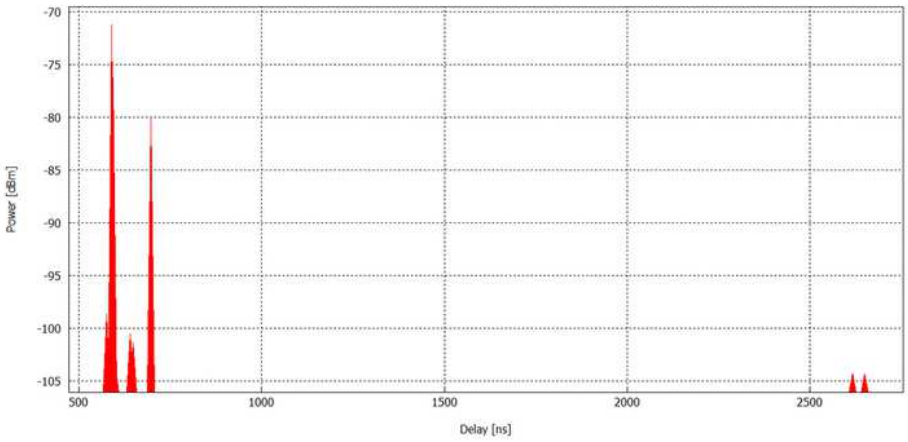

Figure 9

Power delay profile predicted at 0s

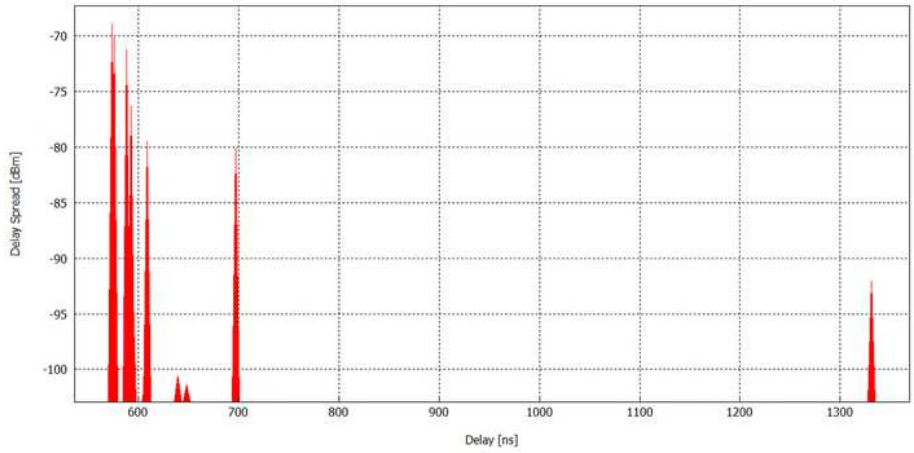

Figure 10

Power delay profile predicted at 3s